

Simulation of ECT Bobbin Coil Probe Signals to Determine Optimum Coil Gap

Young Bae Kong*[†], Sung-Jin Song*, Chang-Hwan Kim*, Hyung-Ju Yu*,
Min Woo Nam**, Dong Hyun Jee** and Hee Jong Lee**

Abstract Eddy current testing (ECT) signals produced by a differential bobbin coil probe vary according to probe design parameters such as the number of turns, geometry and coil gap size. In the present study, the characteristics of a differential bobbin coil probe signals are investigated by numerical simulation in order to determine the optimum coil gap. For verification of numerical simulation accuracy, a specially designed bobbin probe of which the coil gap can be adjusted is fabricated and a series of experiments to acquire signals from two kinds of standard tubes with the variation in coil gap is performed. Then, the experimental signals are compared to the simulation results. Based on this investigation, a decision on the optimum range of coil gap is made. The theoretically predicted signals agree very well to the experimental signals. In fact, this excellent agreement demonstrates a high potential of the simulation as a design optimization tool for ECT bobbin probes.

Keywords: Eddy Current Testing, Differential Bobbin Coil, Coil Gap Size, Electromagnetic Numerical Analysis.

1. Introduction

Since steam generator (SG) tubes in nuclear power plants are continuously influenced by high pressure water, steam and mechanical vibration during operation, they are likely to have defects. Therefore, inspecting SG tubes during shut down periods is necessary to prevent problems caused by leakage of primary water. Eddy current testing (ECT) using differential bobbin coils is widely adopted for inspections of SG tubes due to its outstanding capability of non-contact, remote high speed scanning from inside of the tubes. The integrity of these tubes is evaluated based on the characteristics of ECT signals. Probes used in ECT have the strongest effect on the signals among all other factors. Specially, the design parameters of probes such as the number

of turns, geometry and coil gap influence significantly on the signal characteristics. Therefore, in order to obtain proper results from bobbin coil probes, it is necessary to optimize the design parameters of a probe (Electric Power Research Institute, 2005).

Probe design is usually performed based on empirical investigations and experiments. Recently, Nam et al. (Nam et al., 2006) has adopted this approach to determine the optimum design parameters of a bobbin probe for inspecting SG tubes in Korean standard nuclear power plants (KSNP). They have found that the coil gap size between two coils had a strong influence on the signal characteristics. In their work, they were able to determine the optimum coil gap of a bobbin coil probe for inspecting the KSNP SG tubes experimentally (Nam et al.,

2006). Their effort was quite successful, but it was time and cost consuming.

Therefore, it is desired to have alternative approaches by which cost and time for design optimization can be reduced. Among alternative approaches, simulation tools are usually adopted instead of experiments. However, to use simulation tools properly, their accuracy and effectiveness should be verified. This study is to address such a need. In this study, we have adopted the same design optimization problem addressed by Nam et al. (et al., 2006), and carried out a set of parametric study. Then we compared the experimental results with the theoretical predictions made by a commercial simulation tool; VIC-3D (Victor Technologies, 2005) which is based on a volume integral method (Dunbar, 1985) of electromagnetic numerical analysis.

2. Experimental Equipment

2.1 Bobbin Probe

Fig. 1 shows the bobbin probe used in the experiments of this study. This probe has the fixed number of turns and cable length. The number of turns was determined by calculation.

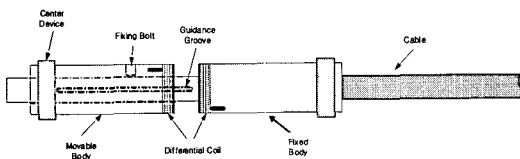


Fig. 1 Bobbin probe for experiments

The probe is composed of a fixed part and a movable part. Thus, the gap between two coils can be adjusted by shifting the movable part. The minimum achievable coil gap of this probe is 0.4 mm. Table 1 summarizes some of the major parameters of the bobbin probe shown in Fig. 1.

2.2 Specimens

For comparison between experiments and simulations, it was desired to have test specimens with flaws on which information was available a priori. For this purpose, we have adopted the ASME and EDM notch standard tubes that are described in EPRI guidelines (Electric Power Research Institute, 2005) as shown in Fig. 2.

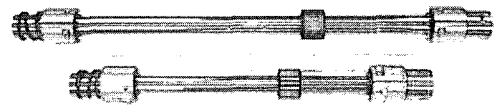


Fig. 2 ASME and notch standard tubes

Among defects in the ASME standard tube, 5 defects of various depths and diameters have been used in this comparison; a 100% through-wall hole (TWH), and four flat bottom holes (FBH) with the depths of 80%, 60%, 40% and 20% of wall thickness. The defects adopted from the EDM notch standard tube are axial and circumferential ID notches of 60 % of wall thickness, 9.5 mm in length and 0.15 mm in width. The notches located at the same axial position, but at opposite side circumferentially. Table 2 summarizes material properties and dimensions of two standard tubes that are made of non-magnetic Inconel 600.

Table 1 Parameters of coil under investigation

	Coil turns	Coil inner diameter	Coil outer diameter	Coil height	Coil thickness	Coil gap
Bobbin coil	60	6.2 mm	7.5 mm	1.3 mm	1.55 mm	0.4 mm~3.2 mm

Table 2 Material properties and dimensions of the standard tubes

Material	Conductivity (S/m)	Rel. Permeability	Inner radius (mm)	Outer radius (mm)	Thickness (mm)
Inconel 600	9.86E5	1	8.458	9.525	1.067

2.3 Experimental Setup

To acquire and analyze ECT signals from the specimens, an experimental system as shown in Fig. 3 has been set up. The experimental system includes a Miz-30 eddy current instrument made by Zetec Inc. in USA and an Eddynet software developed by Zetec Inc.

The experimental system has an automated linear translation scanner that can move the probe with a constant speed of 24 inch/second and sample data with the rate of 1600 sample/second. The primary operation frequency of this system is 550 kHz which is currently adopted for inspecting the KSNP SG tubes.

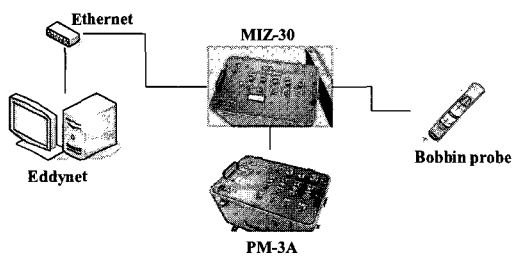


Fig. 3 Test system configuration for eddy current measurement

3. Simulation Setup

For simulation of ECT signals acquired from the standard tubes using bobbin probes, we used commercial software that has been developed based on the volume integral method (Dunbar, 1985). The volume integral method is an effective approach for computing problems associated with eddy current measurement. By adopting an appropriate Green's function for a specimen, this method can effectively reduce time for performing integration to calculate electric field strength. However, this approach often loses accuracy when it is applied to problems with complexity in geometry or material properties (Yoo et al., 2005). In the present study, simulations are carried out based on a set of input parameters such as an operation frequency,

bobbin coil dimensions as shown in Table 1 and properties and dimensions of the standard tubes as shown in Table 2.

4. Comparison between Simulation and Experiment

4.1 ASME Standard Tube

To compare the experimental signals with the theoretical ones, we obtained the data from the TWH, 80%, 60% and 40% FBHs in the ASME standard tube with various coil gaps. It is recognized that voltage peak-to-peak (V_{pp}) measurement is proper than a maximum rate measurement for analysis of ECT signals in many practical cases (Nam et al., 2006). Therefore, we have defined rotational calibration factors to make the V_{pp} phase angles of TWH signals obtained by both experiment and simulation 40° with a coil gap of 0.4 mm and normalized all signals acquired from other three flaws using these pre-defined rotational calibration factors.

One of the desired characteristics of ECT signals obtained by a bobbin probe is that the "center line" connecting the two peaks of lissajous signal is straight. As shown in Fig. 4, when a coil gap is 0.4 mm, the center line of signal is not completely straight but slightly convex. For the coil gaps of between 1.2 mm and 1.6 mm, the center lines are almost straight. However, as the coil gap increases to 2.0 mm and above, the center lines become concave. Fig. 5 shows the results of simulation for the problem discussed in Fig. 4. As shown in Fig. 5, the simulated signals for the TWH agree well to the experimental results. From these experimental results, one can determine that the optimum coil gap in the case of inspecting this TWH would be between 1.2 mm and 1.6 mm.

From Figs. 4 and 5, one can also notice some interesting effects of the coil gap on the signal characteristics. The first effect is that as increase of the coil gap the impedance plane trajectory loses its differential nature since two

coils become distinct absolute probes and the loops become narrower. The second one is that increase of the coil gap causes the phase angles of lissajous signals to rotate clockwise.

Figs. 6 through 11 show comparisons between the experimental signals (Figs. 6, 8, 10) and simulated ones (Figs. 7, 9, 11) obtained from 80%, 60% and 40% FBHs with various coil gaps. From these figures, one can find very good agreements between the experiments and simulations.

In case of 80% and 60% FBHs, the optimum coil gaps are longer than the one for TWH. This implies that the optimum coil gap is related to the size of defect. The changes in signals characteristics such as phase angle, shapes according to the variation of coil gap are very similar in both experiment and simulation.

One of the characteristics imposed by the ASME code on bobbin probes is the phase angle separation between TWH and 20% FBH signals (EPRI, 2005). As shown in the figures, the

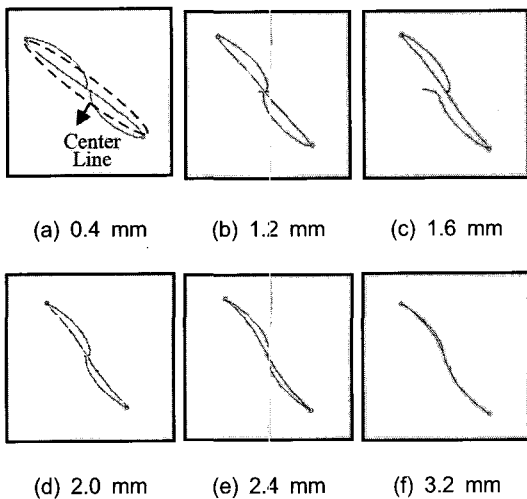


Fig. 4 Lissajous signals acquired from TWH with coil gap variation

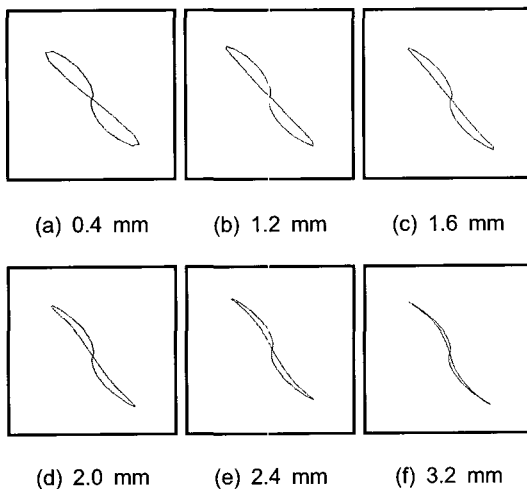


Fig. 5 Lissajous signals simulated from TWH with coil gap variation

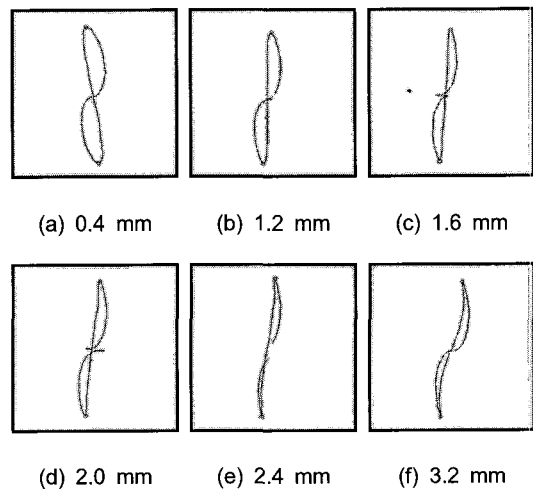


Fig. 6 Lissajous signals acquired from 80% FBH with coil gap variation

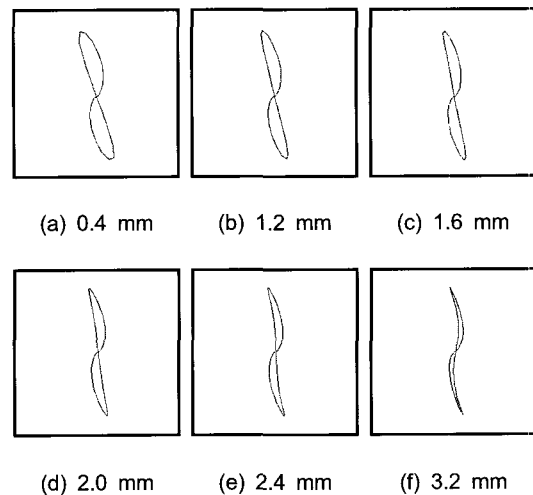


Fig. 7 Lissajous signals simulated from 80% FBH with coil gap variation

separation of the phase angles for both experiments and simulations are from 100° to 110° . This result satisfies the ASME code that requires the phase angle separation of between 50° and 120° . Although the experimental and simulated signals tend to change similarly, discrepancies between the experiment and simulation are observed in phase angle values as shown in Figs. 4 through 11. At this moment, sources of this discrepancy are not fully understood so that further study would be necessary.

4.2 EDM Notch Standard Tube

The electro-discharge machined (EDM) notch standard tube described in EPRI guidelines as shown in Fig. 2 is used to establish setup conditions for rotating pancake coil (RPC) (EPRI, 2005). However, in this study, the ID 60% notches in this tube is used to find the coil gap with which the axial and circumferential notches can be distinguished.

Fig. 12 shows the experimental signals acquired from the EDM notches with various coil gaps.

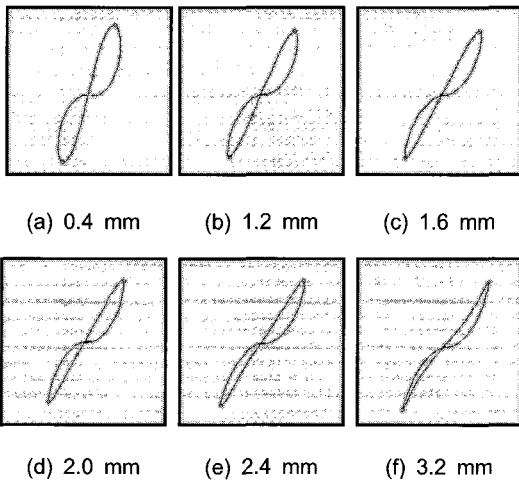


Fig. 8 Lissajous signals acquired from 60% FBH with coil gap variation

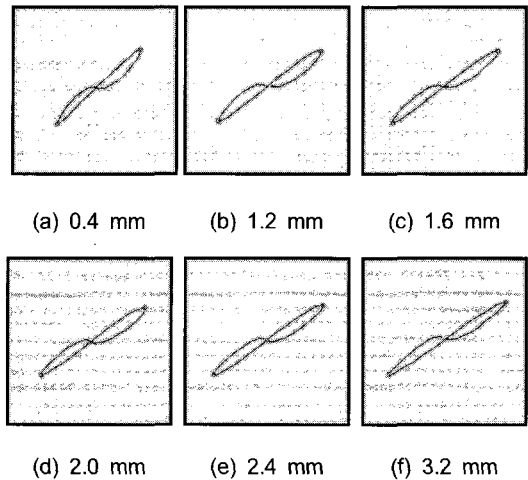


Fig. 10 Lissajous signals acquired from 40% FBH with coil gap variation

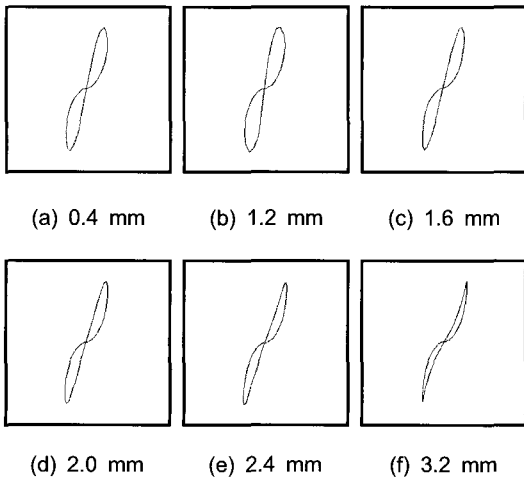


Fig. 9 Lissajous signals simulated from 60% FBH with coil gap variation

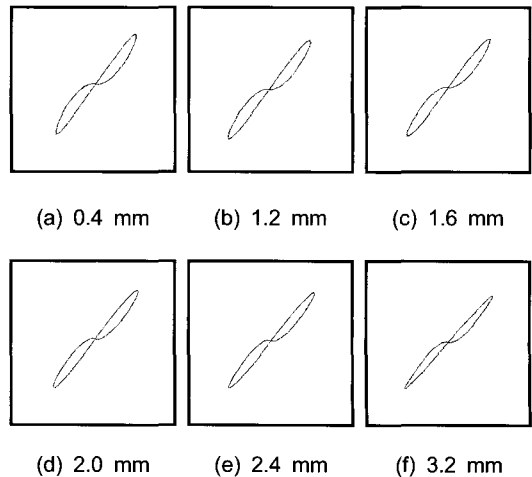


Fig. 11 Lissajous signals simulated from 40% FBH with coil gap variation

The signals shown in this figure can be divided into two parts. The first part is denoted by the solid line circles in expanded strip chart in Fig. 12. It corresponds to the signals mixed by axial and circumferential notches. The second part is shown by the dotted line circles to identify the signals from the axial notch only.

The signals obtained with the coil gaps smaller than 0.8 mm show clear separation of two parts. However, when the coil gaps were larger than 1.6 mm it is not possible to separate

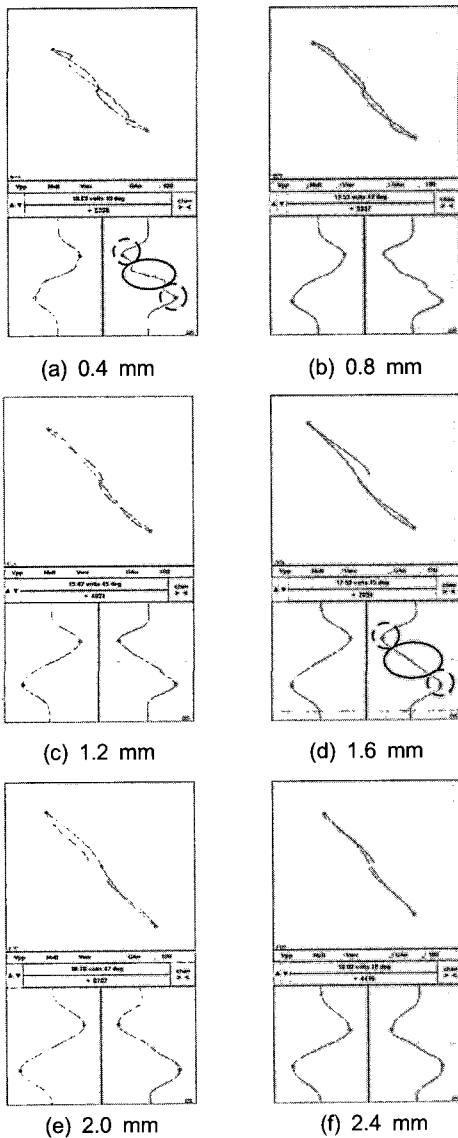


Fig. 12 Lissajous signals acquired from 60% ID EDM notches with coil gap variation

these two parts in expanded strip chart.

To simulate mixed signals from the axial and circumferential notches, we relied on a linearity principle. The signals resulting simultaneously

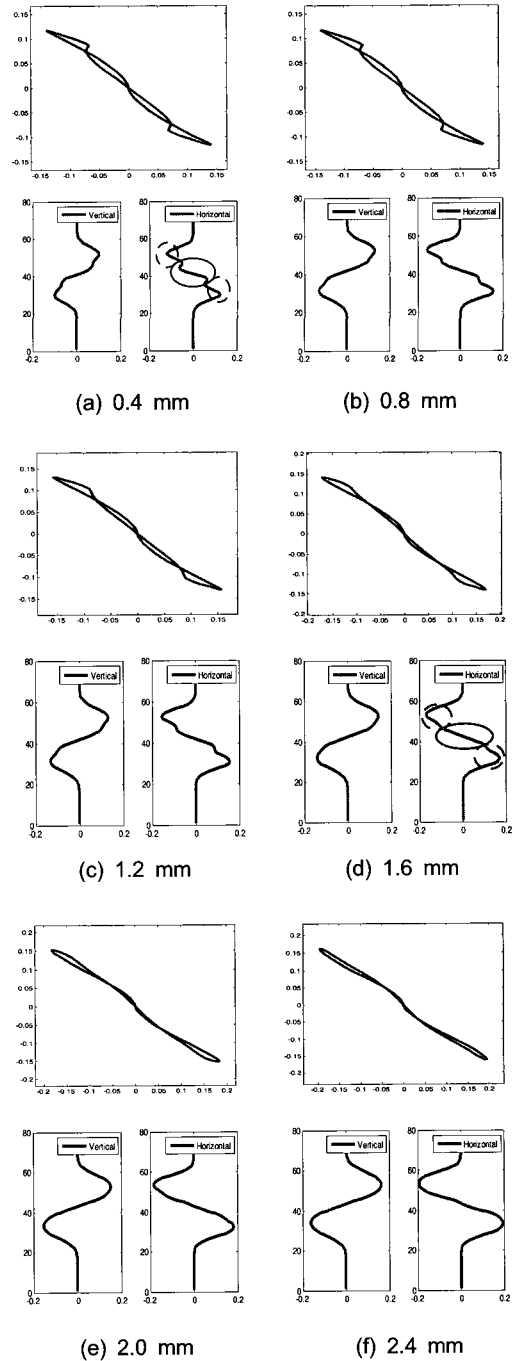


Fig. 13 Lissajous signals simulated from 60% ID EDM notches with coil gap variation

from axial and circumferential defects are equal to the linear combination of the two signals considered separately (ASNT, 1986). Fig. 13 shows the simulated signals for the same problem mentioned at Fig. 12. Comparison of the results shown in Figs. 12 and 13 shows that the linearity principle worked in this case, and demonstrates a high potential of the simulation as a tool for design optimization of the bobbin probe.

5. Simulation for Axial Notches

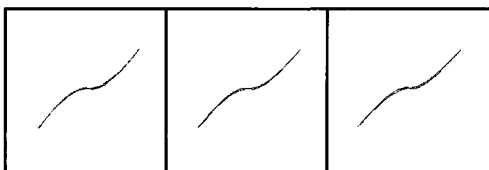
In ECT of SG tubes, the depth of a flaw is evaluated using a phase-depth calibration curve. If the depth of defect is bigger than the 40% thickness of tubes the tubes are to be plugged generally. Using the optimum coil gap obtained in Section 4.1, we predicted the results for



(a) notch length 5 mm, coil gaps=1.2, 1.6, 2.0 mm from left to right



(b) notch length 7 mm, coil gaps=1.2, 1.6, 2.0 mm from left to right



(c) notch length 9 mm, coil gaps=1.2, 1.6, 2.0 mm from left to right

Fig. 14 Lissajous signals simulated from three axial notches with different lengths

various defect lengths which are larger than the 40% FBH. Table 3 shows the parameters of the axial defects and the coil gaps used in this simulation.

Table 3 Parameters of the axial defects

	A	B	C
Depth	40% OD (0.427 mm)		
Width	0.15 mm		
Length	5 mm	7 mm	9 mm
Coil gaps	1.2 / 1.6 / 2.0 mm		

From Fig. 14, we can notice some interesting effects of the defect length on the signal characteristics. In the case with the defect length of 5 mm, the center line is slightly convex. In Section 4.1, it is pointed out that the coil gap was smaller than the defect size, the center line also became convex. However, as the defect length increased above 5 mm, the center lines of the lissajous signals become concave. From this result, one can determine that the center line between the two peaks is not straight or convex when the defect size is much bigger than the coil gap.

6. Summary

In this study, we have considered a design problem of a bobbin probe with an emphasis on finding the optimum coil gap. We have used a specially fabricated bobbin probe of which the coil gap can be adjusted and carried out the experiments to acquire signals from two types of standard tubes with the coil gap variation. Then, the experimental signals were compared to the theoretical predictions simulated by a commercial electromagnetic numerical analysis tool.

With the coil gap variation, we have investigated the signal characteristics as following: the center line straightness between two peaks of lissajous signal, phase angle rotation as coil gap variation and separation of the axial/circumferential defects. From these

characteristics, the optimum range of the coil gap was determined. In this study, the theoretically predicted signals by an electromagnetic numerical simulation agreed very well to the experimental signals. In fact, these good agreements demonstrate the high potential of the simulation as a practical tool for a design problem of the ECT bobbin probes

Applying the optimum coil gap obtained in these work, we obtained the signals simulated from various defect lengths with larger size than 40% FBH and 40% wall thickness. From this result, one can determine that the center line between the two peaks is not formed as a straight or convex line when the defect size is larger than the coil gap.

Acknowledgements

This work was supported by grant No. R-2004-1-138 from the MOCIE (Ministry of Commerce, Industry and Energy).

References

Electric Power Research Institute (2005) Pressurized Water Reactor Steam Generator Examination Guidelines, Revision 6, pp. 720-21

Nam, M. W., Cho, C. H., Jee, D. H., Jung, J. H. and Lee, H. J. (2006) An Analysis of Signal Characteristics due to Coil-Gap Variation of ECT Bobbin Probe for Steam Generator Tube, Proceedings of 2006 Annual Spring Conference of KSNT, pp. 283-290

Victor Technologies (2005) VIC-3D User Manual, Bloomington, Indianapolis

Dunbar, W. S. (1985) The Volume Integral Method of Eddy Current Modeling, Journal of Nondestructive Evaluation, Vol. 5, No. 1, pp. 43-53

Yoo, J. Y., Kim, C. H., Jung, H. J., Song, S. J., Choi, Y. H., Kang, S. C., Song, M. H. and Jung, H. K. (2005) Prediction and Evaluation of Rotating Pancake Coil Probe Signals Simulated from Steam Generator Tubes, D. O. Thompson and D.E. Chimenti (Eds.), Review of Progress in Quantitative Nondestructive Evaluation, Vol. 25A, AIP Conference Proceedings, American Institute of Physics, NY, pp. 383-390

American Society for Nondestructive Testing (1986) Nondestructive Testing Handbook: Vol. 4 Electromagnetic Testing, pp. 593